

New Class of Ruthenium Sulfide Clusters: $\text{Ru}_4\text{S}_6(\text{PPh}_3)_4$, $\text{Ru}_5\text{S}_6(\text{PPh}_3)_5$, and $\text{Ru}_6\text{S}_8(\text{PPh}_3)_6$

Amanda L. Eckermann, Markus Wunder, Dieter Fenske, Thomas B. Rauchfuss,* and Scott R. Wilson

Department of Chemistry, University of Illinois at Urbana-Champaign, Urbana, Illinois 61801, and Lehrstuhl für Anorganische Chemie, Universität Karlsruhe, Karlsruhe, Germany

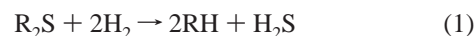
Received January 22, 2002

Reaction of $\text{RuCl}_2(\text{PPh}_3)_3$ with S^{2-} sources yields a family of phosphine-containing Ru–S clusters which have been characterized crystallographically and by MALDI-MS. $\text{Ru}_4\text{S}_6(\text{PPh}_3)_4$ ($\text{Ru}-\text{Ru}_{\text{av}} = 2.94 \text{ \AA}$) has idealized T_d symmetry whereas $\text{Ru}_6\text{S}_8(\text{PPh}_3)_6$ ($\text{Ru}-\text{Ru}_{\text{av}} = 2.82 \text{ \AA}$) adopts the idealized O_h symmetry characteristic of Chevrel clusters. $\text{Ru}_5\text{S}_6(\text{PPh}_3)_5$ is formally derived by the addition of $\text{Ru}(\text{PPh}_3)$ to one face of $\text{Ru}_4\text{S}_6(\text{PPh}_3)_4$. In terms of its M–S connectivity, the Ru_5S_6 cluster resembles a fragment of the FeMo cluster in nitrogenase.

Prototypical Chevrel phases have the empirical formula $M'Mo_6S_8$ ($M' = \text{vacancy or metal cation}$) and are non-molecular solids containing discrete Mo_6 octahedra that are face-capped with chalcogen atoms, some of which also bridge between clusters.¹ Chevrel and Sergent have shown that the Mo_6E_8 cluster ($E = \text{S, Se, Te}$) is but a terminal member of a family of cluster-oligomers. Molecular Chevrel clusters of the formula $M_6E_8L_6$, where L is a terminally bound organic ligand (e.g., PR_3 , amines), have been obtained via excision from Chevrel phase solids² by sulfidation of Mo_6Cl_{12} ^{3,4} and, especially for other metals (Cr,⁵ Fe,⁶ Co^{7,8}), by condensation routes from low nuclearity precursors.

Chevrel clusters have attracted recent attention because of their use in the synthesis of novel porous solids.^{9–11}

Furthermore, McCarley and Schrader showed that PbMo_6S_8 and related species are particularly active catalysts for hydrodesulfurization (HDS) (eq 1), desulfurizing thiophene $> 10\times$ faster than MoS_2 .^{12–14} The enhanced HDS activity of



the Chevrel-based catalysts can be ascribed to their high surface areas. The proportion of edge sites is far greater in cluster-based materials than in MoS_2 -derived materials, in which catalysis is associated with the edge sites.¹⁵ The Chevrel clusters, with S/Mo ratio of 1.33, should be superior S-atom abstracting agents relative to MoS_2 . Furthermore, Chianelli has reported that the sulfides of ruthenium exhibit exceptional HDS activity.¹⁶ This background (the high HDS activity of Mo–S Chevrel phases and RuS_x phases combined with the discovery of molecular Chevrel clusters) leads logically to an interest in Ru-based Chevrel clusters. Although Ru-substituted Chevrel phases of the formula $\text{Ru}_x\text{M}_{6-x}\text{E}_8$ ($M = \text{Nb, Mo}$; $E = \text{Se, Te}$) are known,¹⁷ Ru_6S_8 Chevrel compounds have not been reported.

Treatment of $\text{RuCl}_2(\text{PPh}_3)_3$ with an excess of NaSH in refluxing THF/EtOH afforded a dark precipitate that contains $\text{Ru}_4\text{S}_6(\text{PPh}_3)_4$ (**1**). When the reaction is carried out in THF (without EtOH), dark brown homogeneous solutions are produced that also contain **1**. Cluster **1** can be purified by recrystallization from $\text{CH}_2\text{Cl}_2\text{--Et}_2\text{O}$.

* To whom correspondence should be addressed. E-mail: rauchfuz@ux1.cso.uiuc.edu.

- (1) Saito, T. *Adv. Inorg. Chem.* **1997**, *44*, 45–91.
- (2) Mironov, Y. V.; Virovets, A. V.; Naumov, N. G.; Ikorskii, V. N.; Fedorov, V. E. *Chem.—Eur. J.* **2000**, *6*, 1361–1365.
- (3) For example, $\text{Mo}_6\text{S}_8(\text{pyridine})_6$: Hilsenbeck, S. J.; Young, V. G.; McCarley, R. E. *Inorg. Chem.* **1994**, *33*, 1822–1832.
- (4) $\text{W}_6\text{S}_8(4\text{-tert-butylpyridine})_6$: Venkataraman, D.; Rayburn, L. L.; Hill, L. I.; Jin, S.; Malik, A.-S.; Turneau, K. J.; DiSalvo, F. J. *Inorg. Chem.* **1999**, *38*, 828–830.
- (5) $[\text{Cr}_6\text{E}_8(\text{PR}_3)_6]^{n+}$: Tsuge, K.; Imoto, H.; Saito, T. *Bull. Chem. Soc. Jpn.* **1996**, *69*, 627–636.
- (6) $[\text{Fe}_6\text{S}_8(\text{PET}_3)_6]^{m+}$, $n = 0\text{--}4$: Goddard, C. A.; Long, J. R.; Holm, R. H. *Inorg. Chem.* **1996**, *35*, 4347–4354.
- (7) $\text{Co}_6\text{S}_8(\text{CO})_6$: Diana, E.; Gervasio, G.; Rossetti, R.; Valdemarin, F.; Bor, G.; Stanghellini, P. L. *Inorg. Chem.* **1991**, *30*, 294–299.
- (8) $[\text{Co}_6\text{S}_8(\text{PET}_3)_6]^{+0}$: Cecconi, F.; Ghilardi, C. A.; Midollini, S. *Inorg. Chim. Acta* **1982**, *64*, L47–L48. Cecconi, F.; Ghilardi, C. A.; Midollini, S.; Orlandini, A.; Zanello, P. *Polyhedron* **1986**, *5*, 2021–2031.

- (9) Imoto, H.; Naumov, N. G.; Virovets, A. V.; Saito, T.; Fedorov, V. E. *J. Struct. Chem.* **1999**, *39*, 720–727.
- (10) Naumov, N. G.; Virovets, A. V.; Podberezskaya, N. V.; Fedorov, V. E. *J. Struct. Chem.* **1998**, *38*, 857–862.
- (11) Shores, M. P.; Beauvais, L. G.; Long, J. R. *J. Am. Chem. Soc.* **1999**, *121*, 775–779.
- (12) McCarty, K. F.; Anderegg, J. W.; Schrader, G. L. *J. Catal.* **1985**, *93*, 375–387.
- (13) Hilsenbeck, S. J.; McCarley, R. E.; Thompson, R. K.; Flanagan, L. C.; Schrader, G. L. *J. Mol. Catal. A: Chem.* **1997**, *122*, 13–24.
- (14) Hilsenbeck, S. J.; McCarley, R. E.; Goldman, A. I.; Schrader, G. L. *Chem. Mater.* **1998**, *10*, 125–134.
- (15) Daage, M.; Chianelli, R. R. *J. Catal.* **1994**, *149*, 414–427.
- (16) (a) Pecoraro, T. A.; Chianelli, R. R. *J. Catal.* **1981**, *67*, 430–445. (b) Berhault, G.; Maugé, F.; Lavalley, J.-C.; Lacroix, M.; Breysse, M. J. *Catal.* **2000**, *189*, 431–437.
- (17) For leading references, see: Neuhausen, J.; Finckh, E. W.; Kremer, R. K.; Tremel, W. *Inorg. Chem.* **1996**, *35*, 5622–5626.

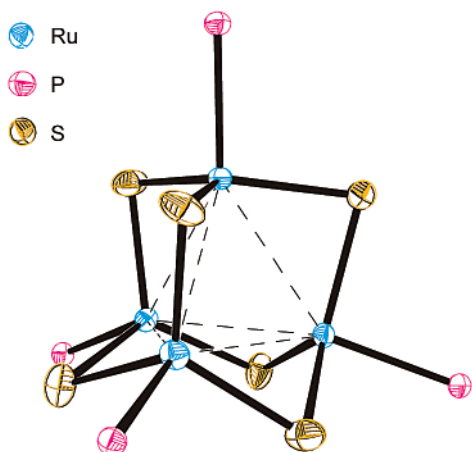


Figure 1. Thermal ellipsoid plot of $\text{Ru}_4\text{S}_6(\text{PPh}_3)_4$ (**1**) drawn at 35% probability level. Hydrogen and carbon atoms are omitted for clarity. Average distances (\AA): Ru–Ru = 2.94; Ru–P = 2.31; Ru–S = 2.21.

Solutions of **1** exhibit no discernible ^{31}P NMR signal, a fact that initially hindered progress on this project. Evans NMR measurements confirm that **1** is paramagnetic, with a moment of $1.88 \mu_{\text{B}}$ at room temperature. We have found that MALDI mass spectrometry can be used for assaying reaction mixtures. Strong molecular ion currents for $[\text{Ru}_4\text{S}_6(\text{PPh}_3)_{4-x}]^+$ ($x = 0, 1, \text{ and } 2$) are observed when exciting at $\lambda = 337 \text{ nm}$ using HABA (2-(4-hydroxyphenyl)-azobenzoic acid) as the matrix. Our experiments revealed that **1** is consistently produced by the $\text{RuCl}_2(\text{PPh}_3)_3/\text{NaSH}$ reaction.

Crystallographic analysis established that **1** consists of a tetrahedral Ru_4 core with sulfur atoms bridging each of the six edges (Figure 1). The Ru–Ru distances of 2.95–2.93 \AA are not consistent with strong metal–metal bonding; typical Ru(III)–Ru(III) bonds (in even higher coordination number metal centers) are ~ 2.75 – 2.80 \AA .^{18,19} The Ru–P distances of 2.31 \AA are $\sim 0.04 \text{ \AA}$ shorter than in six-coordinate Ru(III)– PPh_3 species. The geometry around each Ru center may best be described as flattened tetrahedral, each Ru being only 0.26 \AA above the plane containing the three sulfur atoms to which it is bonded ($\Sigma_{\text{S–Ru–S}} = 356^\circ$). The short Ru–S distances of 2.2 \AA in **1** are consistent with some multiple bonding (π -donation from S to Ru), although short distances are also characteristic of the low coordination number of the Ru centers. As a consequence of sustained efforts to optimize the synthesis of **1**, we have crystallized **1** in three space groups, although the resulting structures are very similar.²⁰ Clusters with M_4S_6 cores are rare: the best precedent to **1** is $\text{W}_4\text{S}_6(\text{PMe}_2\text{Ph})_4$ ($r_{\text{W–W}} = 2.63 \text{ \AA}$), generated in low yield by the Na(Hg)-reduction of $\text{W}_4\text{S}_6\text{Cl}_2(\text{PMe}_2\text{Ph})_4$.²¹ The cluster $\text{W}_4\text{S}_6(\text{PMe}_2\text{Ph})_4$ has 12 d-electrons compatible with 6 W–W bonds; in contrast, **1** with 20 d-electrons shows correspondingly weakened $\text{Ru}\cdots\text{Ru}$ interactions. Cyclic voltammetry

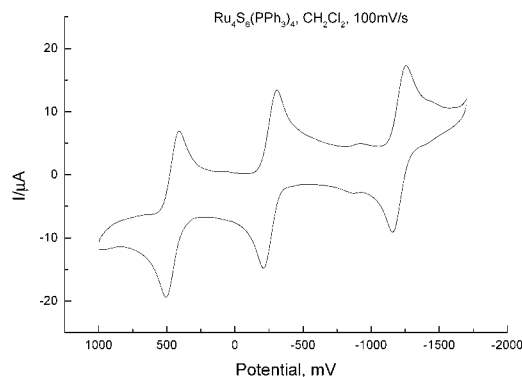


Figure 2. Cyclic voltammogram of $\text{Ru}_4\text{S}_6(\text{PPh}_3)_4$ (**1**) in CH_2Cl_2 vs Ag/AgCl with NBu_4PF_6 as supporting electrolyte.

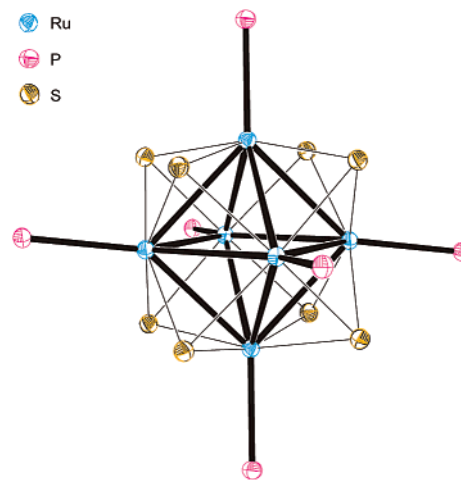


Figure 3. Thermal ellipsoid plot of $\text{Ru}_6\text{S}_8(\text{PPh}_3)_6$ (**2**) drawn at 35% probability level. Hydrogen and carbon atoms are omitted for clarity. Average distances (\AA): Ru–Ru = 2.82; Ru–S = 2.37; Ru–P = 2.31.

measurements show that **1** is electron-rich ($E_{1/2} = +454, -263, -1209 \text{ mV}$ vs Ag/AgCl) and undergoes three reversible redox changes (Figure 2).

Compound **1** reacts with water, and for this reason, silica gel should be dried before chromatographic purification of **1**. MALDI-MS analysis of hydrolyzed samples featured peaks assignable to $\text{Ru}_4\text{S}_5\text{O}(\text{PPh}_3)_4$ and $\text{Ru}_4\text{S}_4\text{O}_2(\text{PPh}_3)_4$.

The cluster $\text{Ru}_6\text{S}_8(\text{PPh}_3)_6$ (**2**) crystallized in $\sim 12\%$ yield from the reaction solutions that also produce **1**. Using pure ethanol as the reaction solvent increased the yield to $\sim 50\%$. Parallel studies using $\text{Se}(\text{TMS})_2$ ($\text{TMS} = \text{Si}(\text{CH}_3)_3$) as a source of Se^{2-} suggest that the condensation approach enjoys some generality; for example, we have prepared $\text{Ru}_6\text{Se}_8(\text{PPh}_3)_6$ and $[\text{Ru}_6\text{Se}_8(\text{PPh}_3)_6]^{2+}$ by a similar route.²² The structure of **2** was confirmed by analysis of crystals in two different space groups, both of which gave very similar metrical results.²³ As in other Chevrel clusters, the Ru atoms in **2** are arranged in an octahedron with each of the faces capped with μ_3 -sulfur atoms (Figure 3). The average Ru–Ru distance in **2**, which has 32 d-electrons, is 2.83 \AA . In

(18) Amarasekera, J.; Rauchfuss, T. B.; Wilson, S. R. *J. Chem. Soc., Chem. Commun.* **1989**, 14, 14–16.

(19) Feng, Q.; Rauchfuss, T. B.; Wilson, S. R. *J. Am. Chem. Soc.* **1995**, 117, 4702–4703.

(20) The cell constants and a brief description of these systems is provided in the Supporting Information.

(21) Kuwata, S.; Mizobe, Y.; Hidai, M. *J. Chem. Soc., Dalton Trans.* **1997**, 1753–1758.

(22) The reaction of $\text{RuCl}_2(\text{PPh}_3)_3$ with $\text{Se}(\text{TMS})_2$ gives $\text{Ru}_6\text{Se}_8(\text{PPh}_3)_6$ and, in the presence of KPF_6 , $[\text{Ru}_6\text{Se}_8(\text{PPh}_3)_6](\text{PF}_6)_2$ (Ru–Ru = 2.80 \AA , Ru–Se = 2.47 \AA , Ru–P = 2.37 \AA).

(23) Crystals of compound **2** have been grown in two space groups. The cell constants and descriptions of methods of crystallization are provided in the Supporting Information.

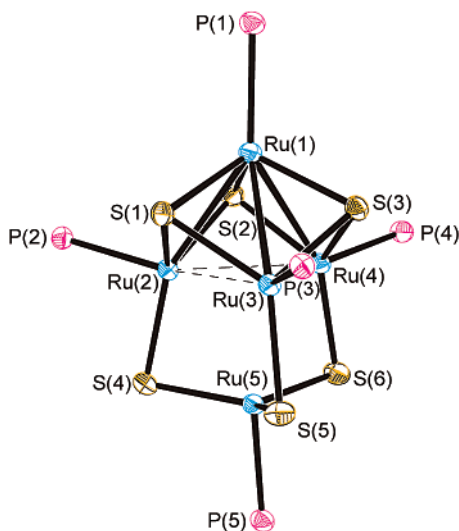
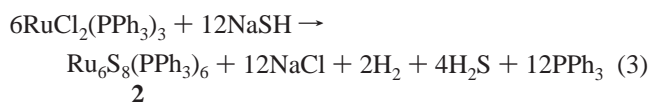
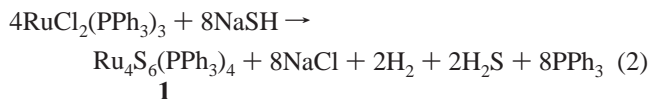


Figure 4. Thermal ellipsoid plot of $\text{Ru}_5\text{S}_6(\text{PPh}_3)_5$ (**3**) (35% probability). Hydrogen and carbon atoms are omitted for clarity. Average distances (Å): $\text{Ru}(1)\text{--Ru}(2,3,4) = 2.79$; $\text{Ru}(2,3,4)\text{--Ru}(2,3,4) = 2.93$; $\text{Ru}(5)\text{--Ru}(2,3,4) = 3.02$; $\text{Ru}(1)\text{--P}(1) = 2.36$; $\text{Ru}(2,3,4)\text{--P}(2,3,4) = 2.30$; $\text{Ru}(5)\text{--P}(5) = 2.27$; $\text{Ru}(1)\text{--S}(1,2,3) = 2.24$; $\text{Ru}(2,3,4)\text{--S}(1,2,3) = 2.26$; $\text{Ru}(2,3,4)\text{--S}(4,5,6) = 2.25$; $\text{Ru}(5)\text{--S}(4,5,6) = 2.20$.

contrast, the $\text{W}\text{--}\text{W}$ bond distance in the electron precise 24e cluster $[\text{W}_6\text{Cl}_{14}]^{2-}$ is 2.61 \AA (2.65 \AA in $[\text{Re}_6\text{Se}_8(\text{PEt}_3)_6]^{2+}$).²⁵ A redox series of analogous clusters $\text{Fe}_6\text{S}_8(\text{PEt}_3)_6^n$ ($n = 0\text{--}4^+$) has been explored; the first isolated was $[\text{Fe}_6\text{S}_8(\text{PEt}_3)_6](\text{BF}_4)_2$, synthesized from $[\text{Fe}(\text{OH}_2)_6](\text{BF}_4)_2$, PEt_3 , and H_2S .⁶ Clusters **1** and **2** both feature oxidized Ru relative to the Ru(II) precursor; their formation can be rationalized by the coformation of H_2 (eqs 2 and 3). Cyclic voltammetric measurements of **2** could not be made because of its insolubility in pure form.



Cluster **2** is a rare example of a PPh_3 -ligated Chevrel cluster; most previous examples of molecular Chevrel clusters feature more basic donor ligands (alkyl phosphines, amines, halides). The ability of PPh_3 to stabilize the cluster suggests that the Ru_6S_8 unit is more Lewis acidic than most Chevrel clusters.

Clusters **1** and **2** differ significantly in their susceptibility toward ligand substitution, as analyzed by MALDI-MS. Neat PBU_3 effects only partial substitution in **2**, even after 6 h at $150 \text{ }^\circ\text{C}$. In contrast, addition of excess PBU_3 to a solution of

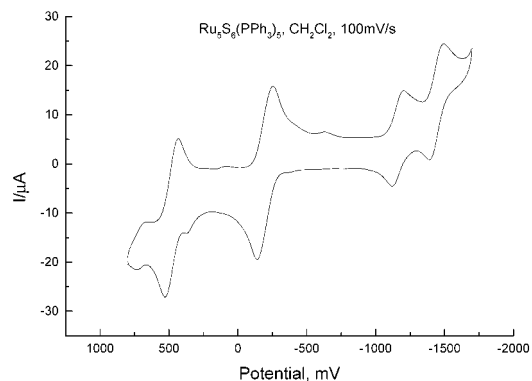


Figure 5. Cyclic voltammogram of $\text{Ru}_5\text{S}_6(\text{PPh}_3)_5$ (**3**) in CH_2Cl_2 vs Ag/AgCl with NBu_4PF_6 as supporting electrolyte.

1 in CH_2Cl_2 ($40 \text{ }^\circ\text{C}$ for 1.5 h) resulted in complete substitution to give $\text{Ru}_4\text{S}_6(\text{PBU}_3)_4$. Cluster **1** does not, however, bind CO, although it is easily oxidized.

MALDI-MS analysis of some preparations of **1** and **2** revealed ions corresponding to $\text{Ru}_5\text{S}_6(\text{PPh}_3)_5$ (**3**). This compound is best prepared by treatment of $\text{RuCl}_2(\text{PPh}_3)_3$ with $\text{S}(\text{TMS})_2$ in hot THF. The Ru centers in **3** are less oxidized than in **1** and **2**; in this case, the reduced product may be $(\text{TMS})_2$ rather than H_2 as in the case of **1** and **2**. Structurally, **3** is related to **1** by capping one of the four faces with a $\text{Ru}(\text{PPh}_3)$ unit (Figure 4). The face capping produces a “Roussin-like” $\text{M}_4(\mu_3\text{-S})_3$ subunit.²⁶ The Ru–Ru distances within this more compact subunit are contracted by $\sim 0.15 \text{ \AA}$ relative to those in **1**, reflecting increased Ru–Ru bonding concomitant with the appearance of $\mu_3\text{-S}$ centers. Holm has prepared analogous heterometallic $\text{M}'\text{M}_4\text{S}_5\text{L}_5$ clusters.²⁷

The cyclic voltammogram of **3** displays significant similarities to **1**, featuring apparent $2e$ oxidations at $+479$ and -197 mV and $1e$ reductions at -1159 and -1447 mV (Figure 5).

Cluster **3** may be a precursor to the “anti-Chevrel” cluster $\text{Ru}_8\text{S}_6(\text{PPh}_3)_8$, wherein all four faces of **1** are capped by $\text{Ru}(\text{PPh}_3)$ units. Traces of this Ru_8S_6 cluster are detected in the MALDI mass spectra of some preparations.

In closing, we note that the coformation of three structurally and stoichiometrically related $\text{Ru}(\text{PPh}_3)\text{--S}$ clusters points to the feasibility of deciphering mechanistic interrelationships, which we are currently attempting.

Acknowledgment. This research was supported by the National Science Foundation and the Deutsche Forschungsgemeinschaft. We thank Dr. Joel Dopke for experimental assistance at the early stages of this project.

Supporting Information Available: Experimental section (PDF) and X-ray crystallographic files (CIF). This material is available free of charge via the Internet at <http://pubs.acs.org>.

IC0255104

(24) Zietlow, T. C.; Schaefer, W. P.; Sadeghi, B.; Hua, N.; Gray, H. B. *Inorg. Chem.* **1986**, *25*, 2195–2198.

(25) Zheng, Z. P.; Long, J. R.; Holm, R. H. *J. Am. Chem. Soc.* **1997**, *119*, 2163–2171.

(26) Coucouvanis, D.; Han, J.; Moon, N. *J. Am. Chem. Soc.* **2002**, *124*, 216–224.

(27) (a) Nordlander, E.; Lee, S. C.; Cen, W.; Wu, Z. Y.; Natoli, C. R.; Di Cicco, A.; Filippini, A.; Hedman, B.; Hodgson, K. O.; Holm, R. H. *J. Am. Chem. Soc.* **1993**, *115*, 5549–5558. (b) Cen, W.; MacDonnell, F. M.; Scott, M. J.; Holm, R. H. *Inorg. Chem.* **1994**, *33*, 5809–5818. (c) Huang, J.; Mukerjee, S.; Segal, B. M.; Akashi, H.; Zhou, J.; Holm, R. H. *J. Am. Chem. Soc.* **1997**, *119*, 8662–8674.